Extension of a fourth-order damage theory to anisotropic history: Application to ceramic matrix compostites under a multi-axial non-proportional loading

Emmanuel Baranger

Journal Title
XX(X):2–17

DOI: 10.1177/ToBeAssigned
www.sagepub.com/
SAGE

Extension of a 4th order damage theory to anisotropic history: application to CMCs under a multi-axial non-proportional loading

Emmanuel Baranger [1]

Abstract

Ceramic matrix composites have good thermo-mechanical properties at high or very high temperatures. The alliance of two brittle materials (SiC fibers and SiC matrix e.g.) via an interface allows a pseudo-ductile macroscopic behavior due to crack deviation. The modeling of the crack networks using damage mechanics is not straight forward. The main reason is the presence of a crack network oriented by the loading direction, which is not known a priori. The aim of this paper is to extend an anisotropic damage model able to describe such behaviors to multi-axial loadings. For that, compliance-like tensorial damage variables are used in a thermodynamic potential able to account for crack closure effects. The damage kinematic is initially completely free and imposed by the evolution laws. The key point of the present paper is to account for an anisotropic history of damage. The results obtained are put in relation to alternate torsion tests performed on SiC/SiC tubes and richly instrumented.

Keywords

CMC, anisotropic damage, non-proportional loading, 4th order variables, history variable

List of symbols

$\mathbb{C}_0$	Initial compliance tensor
$\Delta\mathbb{C}, \Delta\mathbb{Z}, \Delta\mathbb{C}_m, \Delta\mathbb{Z}_m$	damage compliance tensors
$\mathbb{C} = \mathbb{C}_0 + \Delta\mathbb{C}$	
$\mathbb{H} = \mathbb{C}^{\frac{1}{2}}$ and $\mathbb{H}_0 = \mathbb{C}_0^{\frac{1}{2}}$	
$\rho\Psi^{el}$	State potential ρ is the volumic mass
$< . >_+, < . >_-$	Classical positive and negative parts
$\boldsymbol{\sigma}, \boldsymbol{\sigma}_+, \boldsymbol{\sigma}_-$	Stress, positive part of the stress w.r.t. $\mathbb{H}$ negative part of the stress w.r.t. $\mathbb{H}_0$
$\boldsymbol{\varepsilon}$	Strain
$\mathbb{Y}', \mathbb{Y}', \mathbb{Y}''$	Thermodynamical forces written in stress
$\mathbb{W}', \mathbb{W}', \mathbb{W}''$	Thermodynamical forces written in strain
$\otimes$	Tensor product
:	Contracted product between 2nd order tensors
::	Contracted product between 4th order tensors
$(.)_{sym}$	Symmetric part of a second order tensor
$\mathbb{I}$	Fourth order identity tensor
$\dot{a}$	Total time derivative of a quantity a
$\dot{\omega}$	Dissipated power
a_i	Quantity a evaluated at time step t_i

Introduction

Ceramic matrix composites (CMC) are good candidates for the manufacturing of aeronautical engine structures or nuclear energy applications as they present very good specific properties at high temperatures and irradiations. In both cases, engineers have to dispose of mechanical models in order to design and size parts. Regarding SiC/SiC composites, several crack networks can develop depending on the densification of the material and of the fiber/matrix interface. Among them, inter-yarn cracks may develop orthogonally to the loading directions as mentioned by Aubard (1992).
It has lead to the so-called anisotropic damage models in the literature Kachanov (1992); Ju (1990). The introduction of damage variables to describe the effects of crack networks is generally introduced using the effective stress concept. It has been initiated by Kachanov (1958); Rabotnov (1969) for scalar variables. The problem is more difficult

[1]LMT, ENS-Cachan, CNRS, Université Paris-Saclay, France

Corresponding author:
Emmanuel Baranger, LMT, ENS-Cachan ,CNRS ,Université Paris-Saclay, 61 avenue du président Wilson, F-94235 Cachan, France.
Email: baranger@lmt.ens-cachan.fr

while using tensorial damage variables as in Murakami and Ohno (1981). For example, in Murakami (1988); Betten (1983), a second order damage tensor is used. In order to construct the effective stress, a fourth order effect tensor is built on the basis of this damage description. A difficulty resides in keeping the symmetries of the obtained stress tensor. While an equivalence in strain is generally used, Cordebois and Sidoroff (1979) proposed a solution to that problem assuming an equivalence in energy. This solution has been followed by Voyiadjis and Park (1997) and Park and Voyiadjis (1998) for finite strains. Note that Chaboche (1977) worked on the direct use of a fourth order damage tensor to define an effective stress. Ladevèze (2002) does not use this concept of effective stress.

Another major problem is to account for crack closure effects i.e. restauration of the stiffness in compression. Important for CMCs like in Gasser et al. (1996), this problem of stiffness recovery in compression is also well known in the field of brittle material modeling (Halm and Dragon (1998) for e.g.). The difficulty resides in the obtention of continuous stress/strain relations i.e. convex potential for multi-axial non-proportional loadings Chaboche (1992); Carol and Willam (1996). For that, two main approaches have been developed for CMCs. The first one is to discretize the potential crack directions in the plane and use associated scalar damage variables in fixed directions as in Marcin et al. (2011); Bernachy-Barbe et al. (2015a). The second one is to use tensorial damage variables. The simplest approach is to use a second order tensor damage variable as in Chaboche and Maire (2001); Gasser et al. (1996). Several difficulties associated to the model of Chaboche and Maire are mentioned in Cormery and Welemane (2002) and by the authors themselves. Another approach is to use directly fourth order tensors as in Chaboche (1982). For example, Ladevèze (2002) used compliance tensors as damage variables. He defined associated special positive and negative parts of the stresses in order to get the good properties on the free energy potential Curnier et al. (1994). This model is the basis of this paper. Note that, complex tensorial damage models have been simplified to scalar damage models in the litterature, for example Chaboche and Maire (2001) leads to Marcin et al. (2011). An automatic strategy adapted to that purpose can be found in Baranger (2013); Friderikos and Baranger (2016).

Recent experiences performed at CEA by Bernachy-Barbe et al. (2015b); Bernachy-Barbé (2014), and richly instrumented via digital image correlation, confirm macroscopic observations done by ONERA Maire and Pacou (1996) on tension-torsion tests on SiC/SiC tubes. Concerning the experiments of Bernachy-Barbé, the main crack network is oriented by the loading direction. Therefore, alternate torsion tests leads to the creation of two orthogonal networks oriented by the two main loading directions. It will be shown that the model developed by Ladevèze Ladevèze (2002) is not able to account for such a non-proportional loading as the history is isotropic. Thus, this paper aims at extending this model to account for anisotropic history using concepts developed by Desmorat et al. (2010). Note that similar concepts seems to have been developed by Chaboche while comparing the evolution of his papers Chaboche et al. (1994); Maire and Lesne (1997), but it is not explicitly mentioned by the authors. The identification of such anisotropic models is not straigth-forward. It has been done in Baranger et al. (2008)

based on macroscopic tests and some physical considerations. The rich experimental tests from Bernachy-Barbe et al. (2015b) are a major contribution for that problem.

In this paper, two versions of the original model from Ladevèze (2002) are presented in the next section. Then, predictions of the models are compared to some experimental results to determine whether the models are able to describe the crack orientations (section 3). In section 4, it will be shown that the models are unable to represent non-proportionnal loadings because the history description is isotropic. Based on this, the models are enhanced to account for anisotropic histories and validated (section 5). This last part is the main contribution of this paper.

Original damage model

In order to introduce versatile damage kinematics, different authors have chosen to describe damage using fourth order tensors Chaboche (1982); Ju (1990). In this part, the model from Ladevèze for SiC/SiC composites is emphasized Ladevèze (2002); Cluzel et al. (2009); Genet et al. (2014). The first main idea of this model is to let the damage kinematic completely free a priori and to specify it using the evolution laws. The second idea is to separate the contributions of the different crack networks. The objective is to have a mechanical model that could be linked to physico-chemical one to treat self-healing aspects of lifetime predictions Cluzel et al. (2009); Genet et al. (2012).

State potential and damage variables

The elastic potential $\rho\Psi^{el}$ is written in stress as the sum of three contributions: the first is a contribution only active in tension, the second is a contribution active only in compression and the third is a contribution active both in tension and compression (i.e. mainly shear). It reads:

$$\rho\Psi^{el} = \frac{1}{2}\boldsymbol{\sigma}_+ : \mathbb{C} : \boldsymbol{\sigma}_+ + \frac{1}{2}\boldsymbol{\sigma}_- : \mathbb{C}_0 : \boldsymbol{\sigma}_- + \frac{1}{2}\boldsymbol{\sigma} : \Delta\mathbb{Z} : \boldsymbol{\sigma} \tag{1}$$

$\Delta\mathbb{C} = \mathbb{C} - \mathbb{C}_0$ and $\Delta\mathbb{Z}$ are the damage variables of the model, by definition they are positive and have the symmetries of a compliance tensor so that their square roots $\mathbb{H}$ and $\mathbb{H}_0$ exist. $\boldsymbol{\sigma}_+$ and $\boldsymbol{\sigma}_-$ are positive and negative parts of the stress $\boldsymbol{\sigma}$ defined to manage unilateral contact in cracks (the shear stiffness recovery is not taken into account in this form as it is linked to friction) and to keep a convex potential even for non-proportional loadings. For that, two spectral decompositions are used. The first is used to define the positive part:

$$\boldsymbol{\sigma}_+ = \mathbb{H}^{-1} :< \mathbb{H} : \boldsymbol{\sigma} >_+ \tag{2}$$

The second is used to define the negative part:

$$\boldsymbol{\sigma}_- = \mathbb{H}_0^{-1} :< \mathbb{H}_0 : \boldsymbol{\sigma} >_- \tag{3}$$

For diagonal compliance tensors, these positive and negative parts are equal to the classical one but not in the general case. The use of classical positive and negative parts would lead to a non-convex potential and therefor to non-continuous stress-strain relation. This is due to the presence of terms mixing eigenvalues as shown in Ladeveze (1983). With the proposed positive and negative parts, the state potential is convex with respect to $\boldsymbol{\sigma}$ as demonstrated in Ladevèze et al. (2014). It allows to get a continuous stress-strain relation even during crack closure.The stress-strain relation is given by (see appendix of Baranger (2013) for some calculus elements):

$$\boldsymbol{\varepsilon} = \frac{\partial \rho \Psi^{el}}{\partial \boldsymbol{\sigma}} = \mathbb{C} : \boldsymbol{\sigma}_+ + \mathbb{C}_0 : \boldsymbol{\sigma}_- + \Delta\mathbb{Z} : \boldsymbol{\sigma} \tag{4}$$

The total damage is separated in different contributions related to the different crack networks (inter-yarn cracks, intra longitudinal yarn cracks, intra transverse cracks for example) as in Cluzel et al. (2009). The total damage is the sum of the different contributions. For the sake of simplicity and due to the mechanical properties of the material characterized by Bernachy-Barbe et al. (2015b), in the present paper, the damage is reduced to the inter-yarn cracking network (noted with underscore m). The associated damage contributions are called: $\Delta\mathbb{C}_m$ and $\Delta\mathbb{Z}_m$ while in Cluzel et al. (2009) other contributions are added. Therefor:

$$\Delta\mathbb{C} = \Delta\mathbb{C}_m \tag{5}$$

$$\Delta\mathbb{Z} = \Delta\mathbb{Z}_m \tag{6}$$

Thermodynamical forces

The thermodynamical forces associated to the damage variables are also fourth order tensors:

$$\mathbb{Y} = \frac{\partial \rho \Psi^{el}}{\partial \Delta\mathbb{Z}} = \frac{1}{2}\boldsymbol{\sigma} \otimes \boldsymbol{\sigma} \tag{7}$$

$$\mathbb{Y}' = \frac{\partial \rho \Psi^{el}}{\partial \Delta\mathbb{C}} = \frac{1}{2}\boldsymbol{\sigma}_+ \otimes \boldsymbol{\sigma}_+ \tag{8}$$

Another force is introduced to deal with shear, in 2D:

$$\mathbb{Y}'' = \frac{1}{2}(\boldsymbol{R}_{\frac{\pi}{2}}.\boldsymbol{\sigma}_+)_{sym} \otimes (\boldsymbol{R}_{\frac{\pi}{2}}.\boldsymbol{\sigma}_+)_{sym} \tag{9}$$

where $\boldsymbol{R}_{\frac{\pi}{2}}$ is a $\frac{\pi}{2}$ rotation in the plane.

Several other thermodynamical forces are also introduced. While the previous ones (noted with $\mathbb{Y}$) rely on the stress, the following ones (noted $\mathbb{W}$) rely on the strain. They read:

$$\mathbb{W} = \frac{1}{2}(\mathbb{C} : \boldsymbol{\sigma}) \otimes (\mathbb{C} : \boldsymbol{\sigma}) \tag{10}$$

$$\mathbb{W}' = \frac{1}{2}(\mathbb{C} : \boldsymbol{\sigma}_+) \otimes (\mathbb{C} : \boldsymbol{\sigma}_+) \tag{11}$$

$$\mathbb{W}'' = \frac{1}{2}(\boldsymbol{R}_{\frac{\pi}{2}}.(\mathbb{C} : \boldsymbol{\sigma}_+))_{sym} \otimes (\boldsymbol{R}_{\frac{\pi}{2}}.(\mathbb{C} : \boldsymbol{\sigma}_+))_{sym} \tag{12}$$

Damage evolution laws

To build the damage evolution laws, an equivalent driving force is introduced as:

$$z_m(\mathbb{A}) = \left((1-a)Tr[\mathbb{A}^{n+1}] + aTr[\mathbb{A}]^{n+1}\right)^{\frac{1}{n+1}} \tag{13}$$

$$\tag{14}$$

In the following, $\mathbb{A}$ will be either $\mathbb{Y}'$ or $\mathbb{W}'$. a allows to pass from isotropic to anisotropic damage and n allows to emphasis the directionality of damage. If n is odd, then z_m is positive.

The maximum force over time is defined by:

$$\bar{z}_m(t) = \sup_{\tau \leq t} z_m(\mathbb{A}(\tau)) \tag{15}$$

Regarding the evolution laws, several choices can be found in the literature.

Model (1) In Ladevèze (2002), the damage is driven by the stress. This model is noted (1), the evolution laws read:

$$\Delta\dot{\mathbb{C}}_m = \dot{\alpha}_m \frac{(1-a)\mathbb{Y}'^n + aTr[\mathbb{Y}']^n\mathbb{I}}{\bar{z}_m^n} \tag{16}$$

$$\Delta\dot{\mathbb{Z}}_m = \dot{\alpha}_m \frac{b\mathbb{Y}''^n}{\bar{z}_m^n} \tag{17}$$

$$\bar{z}_m(t) = \sup_{\tau \leq t} z_m(\mathbb{Y}'(\tau)) \tag{18}$$

The dissipated power $\dot{\omega}$ reads:

$$\dot{\omega} = \Delta\dot{\mathbb{C}}_m :: \mathbb{Y}' + \Delta\dot{\mathbb{Z}}_m :: \mathbb{Y} \tag{19}$$

Model (2) In Ladevèze et al. (2014), the strain is privileged. This model is noted (2), the evolution laws read:

$$\mathbb{C}^{-1} : \Delta\dot{\mathbb{C}}_m : \mathbb{C}^{-1} = \dot{\tilde{\alpha}}_m \frac{(1-a)\mathbb{W}'^n + aTr[\mathbb{W}']^n\mathbb{I}}{\bar{z}_m^n} \tag{20}$$

$$\mathbb{C}^{-1} : \Delta\dot{\mathbb{Z}}_m : \mathbb{C}^{-1} = \dot{\tilde{\alpha}}_m \frac{b\mathbb{W}''^n}{\bar{z}_m^n} \tag{21}$$

$$\bar{z}_m(t) = \sup_{\tau \leq t} z_m(\mathbb{W}'(\tau)) \tag{22}$$

The form used for the flow rules is related to the dissipated power that reads:

$$\begin{aligned}\dot{\omega} &= \Delta\dot{\mathbb{C}} :: Y' + \Delta\dot{\mathbb{Z}} :: Y \\ &= (\mathbb{C}^{-1} : \Delta\dot{\mathbb{C}} : \mathbb{C}^{-1}) :: \mathbb{W}' + (\mathbb{C}^{-1} : \Delta\dot{\mathbb{Z}} : \mathbb{C}^{-1}) :: \mathbb{W}\end{aligned} \tag{23}$$

For both models, the damage kinematic is imposed by the flow rules. It has to be noted that for $a = 0$, the damage is oriented by $\mathbb{Y}'$ or $\mathbb{W}'$. This choice is retained in the following. $\alpha_m(\bar{z}_m)$ and $\tilde{\alpha}_m(\bar{z}_m)$ are scalar increasing functions. As mentioned in Genet et al. (2014), these two models lead to positive dissipated powers (a demonstration relies on the use of equation 53 in appendix).

Numerical integration

The numerical implementation of such evolution laws requires robust integration schemes as in Genet et al. (2014). Note that, many eigenvalue problems have to be solved due to the positive and negative parts. This is rather time consuming. In the present case, as in Cluzel et al. (2009); Baranger et al. (2011), a very simple explicit scheme is used. The model being written in stress, it is rather easy to use to exploit classical experimental mechanical tests while it is more difficult to use in a finite element framework.

Crack orientations for tensile loadings and localization

First, it is interesting to check if the proposed models, introducing tensorial damage variables, are able to give some information on the crack directions. Experimental data from Bernachy-Barbe et al. (2015b) are used as a reference. These data are obtained from multi-axial loading on SiC/SiC pipes. The principal and secondary crack networks orientations are presented on Figure 1 for several angles of applied uniaxial loads. The orientations are measured using digital image correlation on the surface of the tube at the scale of the reinforcement.

From damage principal directions

For both models (1) and (2), with $a = 0$ and $n = 1$, the damage evolution laws rely on $\mathbb{Y}'$ and $\mathbb{W}'$. In that sens, the description of the mean crack orientations via the damage variables rely on the principal directions of $\boldsymbol{\sigma}_+$ and $\mathbb{C}^2 : \boldsymbol{\sigma}_+$. The directions given by the damage principal directions are plotted on Figure 1. For low applied stress levels, the model (1) leads to a single straight line of slope 1, this is not the case for model (2) which accounts for the initial anisotropy of the material. These simulations are performed at the beginning of damage. It can be seen that the second model is more appropriate to describe the mean crack orientations. Note that this consideration relies on a fine scale description of the matrix as crack orientations are observed at the scale of the reinforcement.

From localization directions

Damage models are well known to present problems of localization. Hereafter, the existence of singular points is studied in a simplified context with $n = 1$ and for pure tensile loadings. In this context, the strain is given by:

$$\boldsymbol{\varepsilon} = \mathbb{C} : \boldsymbol{\sigma}_+ \tag{24}$$

The term $\mathbb{Z} : \boldsymbol{\sigma}$ describes shear contributions and therefor disappeared from the expression of $\boldsymbol{\varepsilon}$. Bifurcation may occur if $\dot{\boldsymbol{\sigma}}_+ = 0$, Therefor the evolution of the strain has to satisfy :

$$\dot{\boldsymbol{\varepsilon}} = \dot{\mathbb{C}} : \boldsymbol{\sigma}_+ \tag{25}$$

For model (1), at constant applied stress, there is no possible evolution of the damage magnitude and orientation i.e. $\dot{\mathbb{C}} = \mathbb{O}$. Bifurcation cannot occur for model (1).

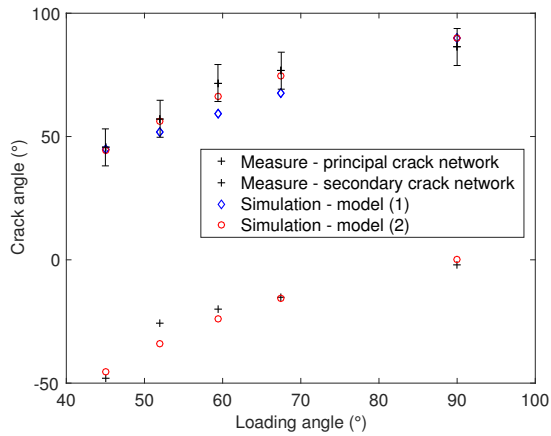

Figure 1. Crack angles vs. loading angle.

For model (2), replacing the damage evolution law leads to:

$$\dot{\boldsymbol{\varepsilon}} = \left(\frac{\dot{\bar{\alpha}}_m}{2} (\mathbb{C}^2 : \boldsymbol{\sigma}_+) \otimes (\mathbb{C}^2 : \boldsymbol{\sigma}_+) \right) : \boldsymbol{\sigma}_+ \tag{26}$$

$$= \left(\frac{\dot{\bar{\alpha}}_m}{2} (\mathbb{C} : \boldsymbol{\varepsilon}) \otimes (\mathbb{C} : \boldsymbol{\varepsilon}) \right) : \boldsymbol{\sigma}_+ \tag{27}$$

$$= \frac{\dot{\bar{\alpha}}_m}{2} (\mathbb{C} : \boldsymbol{\varepsilon}) \, (\boldsymbol{\varepsilon} : \mathbb{C} : \boldsymbol{\sigma}_+) \tag{28}$$

At constant applied stress, $\dot{\bar{\alpha}}_m$ is not necessarily zero. Bifurcation may occur in the direction given by $\mathbb{C} : \boldsymbol{\varepsilon}$. It is the same as the principal directions of damage for this kind of loadings. Note that localization will lead to a rather difficult identification of the model in the present case. Finding an evolution law leading to a delayed maximum stress level on the stress/strain curve is not an easy task on the experimental data from Bernachy-Barbé. Only a very rough one has been performed.

Limitations of the model for non-proportional loadings

Experimental comparison and model limitations

To test the previous models on non-proportional loadings, alternate shear loadings performed on a $[\pm 45]$ tube under torsion have been used. On Figure 2, the shear stress is plotted versus the axial, hoop and shear strains. For that, Bernachy-Barbé (2014) assumed an homogeneous state of stress and a simple kinematic. The loading consists of different phases. The loading begins by a positive torsion increasing from points O to point A. The torsion is decreased down to O and to B by applying a negative

torsion. The tube is then reloaded by O and A up to C. A positive (resp. negative) shear stress corresponds to a positive (resp. negative) torque. On this figure, the relation of the axial strain and the shear stress relies uniquely on the compliance evolution in the reinforcement directions i.e. to damage evolution $\Delta\mathbb{C}$ projected on the $+45^o$ direction and -45^o direction. Note that the damage does not evolve until the shear stress reaches the absolute value of about 100 MPa. Also note that this figure is symmetric. Two independent orthogonal crack networks are formed in the directions of the reinforcement.

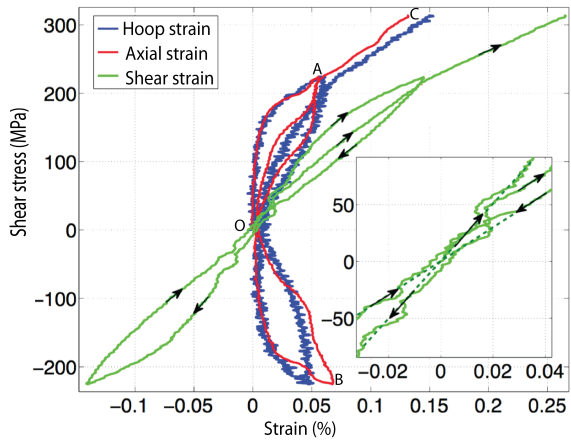

Figure 2. Experimental evolution of the shear stress vs. strain for a pipe loaded in alternate torsion from Bernachy-Barbé (2014).

Figure 3 is a result of a simulation of model (1). It can be noticed that it is not symmetric (regarding the abscissa axis) while the experimental one from Bernachy-Barbé (2014) is (see Figure 2). The same holds for model (2).

Analysis of the history description of the models

Model (1) In fact, $\bar{z}_m(t)$ being a scalar, the damage history is resumed as an isotropic value even if the damage kinematic is very rich. Another way is to note that the damage flow can be rewritten, in a similar manner with the flow rule given by equations 16 and 20.

For model (1), it is simple, it reads:

$$\Delta\dot{\mathbb{C}}_m = \dot{\gamma}\frac{\partial z_m}{\partial \mathbb{Y}'} \tag{29}$$

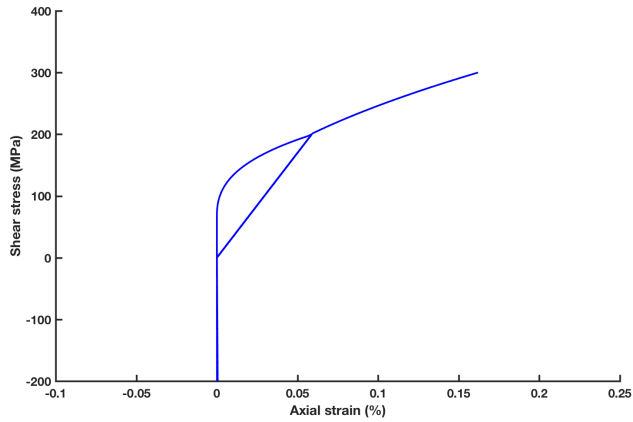

Figure 3. Simulated evolution of the shear stress vs. axial strain for a pipe loaded in alternate torsion.

$\dot{\gamma}$ is a damage multiplier, some Khun-Tucker conditions are associated ($\dot{\gamma} \geq 0, f \leq 0, \dot{\gamma} f = 0$). The criterion of damage reads:

$$f(d_{act}) = d_{act} - \beta_m(z_m) \tag{30}$$

If $d_{act} = Tr[\Delta \mathbb{C}_m]$, the damage multiplier is given by:

$$\dot{\gamma} = \frac{\beta_m(z_m)}{Tr[\frac{\partial z_m}{\partial \mathbb{Y}'}]} = \dot{\alpha}_m \tag{31}$$

This expression depends only on $\mathbb{Y}'$. Thus the model is equivalent to the model (1) presented in the previous section. It is another way to present the isotropic history description of the model.

Model (2) Regarding model (2), it is more difficult. One has to define d_{act} from its evolution law:

$$\dot{d}_{act} = Tr[\mathbb{C}^{-1} : \Delta \dot{\mathbb{C}}_m : \mathbb{C}^{-1}] \tag{32}$$

The flow rule is:

$$\mathbb{C}^{-1} : \Delta \dot{\mathbb{C}}_m : \mathbb{C}^{-1} = \dot{\gamma} \frac{\partial z_m}{\partial \mathbb{W}'} \tag{33}$$

The damage multiplier reads:

$$\dot{\gamma} = \frac{\dot{\beta}_m}{Tr[\frac{\partial z_m}{\partial \mathbb{W}'}]} = \dot{\tilde{\alpha}}_m \tag{34}$$

Once again, it depends only of $\mathbb{W}'$.

Remark: the shear parts of the damage can be rewritten in the same way:

$$\Delta\dot{\mathbb{Z}}_m = \dot{\gamma}\frac{b\mathbb{Y}''^n}{\bar{z}_m^n} \tag{35}$$

$$\mathbb{C}^{-1} : \Delta\dot{\mathbb{Z}}_m : \mathbb{C}^{-1} = \dot{\gamma}\frac{b\mathbb{W}''^n}{\bar{z}_m^n} \tag{36}$$

Enhanced damage model with anisotropic history

Model improvement

As illustrated above, the evolution equations have to be modified to account for anisotropic history. Desmorat et al. (2010) proposed a framework for that on 2D damage tensors. His approach is followed here.

For model (1), one introduces:

$$d_{act} = \Delta\mathbb{C}_m :: \frac{\mathbb{Y}'}{z_m(\mathbb{Y}')} \tag{37}$$

In the following, the damage evolution laws are written at time step t_{i+1}. First, the projection of damage at the current ($d_{act,i+1}$) and previous ($d^*_{act,i+1}$) time steps on the current loading direction read:

$$d_{act,i+1} = \Delta\mathbb{C}_{m,i+1} :: \frac{\mathbb{Y}'_{i+1}}{z_{m,i+1}} \tag{38}$$

$$d^*_{act,i+1} = \Delta\mathbb{C}_{m,i} :: \frac{\mathbb{Y}'_{i+1}}{z_{m,i+1}} \tag{39}$$

The flow rule is written as :

$$(\Delta\mathbb{C}_{m,i+1} - \Delta\mathbb{C}_{m,i}) = \delta\gamma_{i+1}\left(\frac{\partial z_m}{\partial\mathbb{Y}'}\right)_{i+1} \tag{40}$$

Subtracting equations 38 and 39 and introducing the flow rule leads to (see appendix for the simplification):

$$d_{act,i+1} - d^*_{act,i+1} = (\Delta\mathbb{C}_{m,i+1} - \Delta\mathbb{C}_{m,i}) :: \frac{\mathbb{Y}'_{i+1}}{z_{m,i+1}} \tag{41}$$

$$= \delta\gamma_{i+1}\left(\frac{\partial z_m}{\partial\mathbb{Y}'}\right)_{i+1} :: \frac{\mathbb{Y}'_{i+1}}{z_{m,i+1}} \tag{42}$$

$$= \delta\gamma_{i+1} \tag{43}$$

Therefor, if damage increases i.e. $d_{act,i+1} - d^*_{act,i+1} > 0$, then $\delta\gamma_{i+1} \geq 0$ and $d_{act,i+1} = \beta_m(z_{m,i+1})$ and:

$$\Delta\dot{\mathbb{C}}_{m,i+1} = \left(\beta_m(z_{m,i+1}) - d^*_{act,i+1}\right)\left(\frac{\partial z_m}{\partial \mathbb{Y}'}\right)_{i+1} \tag{44}$$

Note that, implicitly, the loading direction is assumed to remain constant over a time step. The dissipated power is positive, the proof is very similar to the one related to the original model.

For model (2), one introduces:

$$d_{act} = \Delta\mathbb{C}_m :: \left(\mathbb{C}^{-1} : \frac{\mathbb{W}'}{z_m(\mathbb{W}')} : \mathbb{C}^{-1}\right) \tag{45}$$

At time step $i+1$:

$$d_{act,i+1} = \Delta\mathbb{C}_{m,i+1} :: \left(\mathbb{C}^{-1}_{i+1} : \frac{\mathbb{W}'_{i+1}}{z_{m,i+1}} : \mathbb{C}^{-1}_{i+1}\right) \tag{46}$$

$$d^*_{act,i+1} = \Delta\mathbb{C}_{m,i} :: \left(\mathbb{C}^{-1}_{i+1} : \frac{\mathbb{W}'_{i+1}}{z_{m,i+1}} : \mathbb{C}^{-1}_{i+1}\right) \tag{47}$$

Subtracting these two expressions and introducing the flow rule leads to (see appendix for the simplification):

$$d_{act,i+1} - d^*_{act,i+1} = \left(\Delta\mathbb{C}_{m,i+1} - \Delta\mathbb{C}_{m,i}\right) :: \left(\mathbb{C}^{-1}_{i+1} : \frac{\mathbb{W}'_{i+1}}{z_{m,i+1}} : \mathbb{C}^{-1}_{i+1}\right) \tag{48}$$

$$= \delta\gamma_{i+1}\left(\mathbb{C}_{i+1} : \left(\frac{\partial z_m}{\partial \mathbb{W}'}\right)_{i+1} : \mathbb{C}_{i+1}\right) :: \left(\mathbb{C}^{-1}_{i+1} : \frac{\mathbb{W}'_{i+1}}{z_{m,i+1}} : \mathbb{C}^{-1}_{i+1}\right) \tag{49}$$

$$= \delta\gamma_{i+1} \tag{50}$$

Therefor, if damage increases i.e. $d_{act,i+1} - d^*_{act,i+1} > 0$, then $d_{act,i+1} = \tilde{\beta}_m(z_{m,i+1})$ and:

$$\mathbb{C}^{-1}_{i+1} : \Delta\dot{\mathbb{C}}_{m,i+1} : \mathbb{C}^{-1}_{i+1} = \left(\tilde{\beta}_m(z_{m,i+1}) - d^*_{act,i+1}\right)\left(\frac{\partial z_m}{\partial \mathbb{W}'}\right)_{i+1} \tag{51}$$

Once again, the dissipated power is positive for the same reason as the original model.

Experimental validation

For alternate shear loadings performed on a $[\pm 45]$ tube under torsion, the shear stress is plotted versus the axial strain on Figure 4 for model (1). It can be noticed that it is now symmetric as for the experimental one Figure 2. Due to localization, it has not

been possible to identify correctly model (2) to illustrate this case on the material from Bernachy-Barbe et al. (2015b). However, Figure 5 gives an illustration of the behavior of a fictitious material. The definition of d_{act} in model (2) introducing the strain, the figure may not be exactly symmetric as the loading is driven by the stress and the damage evolves between the two loading directions at +45 and -45. The first model is easier to use and better suited in this case. Contrary to crack orientations prediction, this time, the description occurs at the macroscopic scale. The two models are thus complementary.

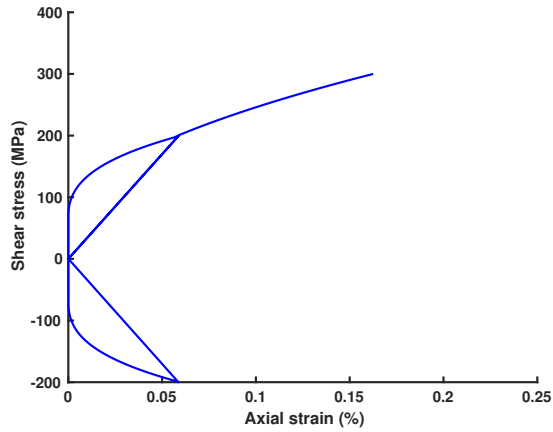

Figure 4. Simulated evolution of the shear stress vs. axial strain for a pipe loaded in torsion for model (1).

Conclusion

In this paper, an anisotropic damage model has been enhanced in order to account for non-proportional loadings. For that, an anisotropic history has been taken into account by projecting the fourth order damage variable on the loading direction. In order to validate the model, simulations have been compared to experimental results at two scales. At fine scale, the model driven by the strain is better suited to describe crack orientations. At the macroscopic scale, on SiC/SiC pipes under alternate torsion, the model driven by the strain is too difficult to identify and only a basic illustration is given. The model driven by the stress shows a good agreement with the experimental data. The on going work focuses on the shear damage deactivation while cracks are in compression.

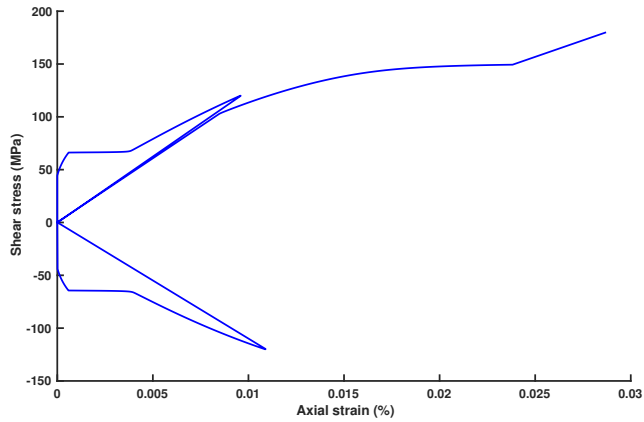

Figure 5. Simulated evolution of the shear stress vs. axial strain for a pipe loaded in torsion for model (2).

Appendix: Damage flow direction

The variation of z_m reads

$$\begin{aligned}\delta z_m =& \frac{\partial z_m}{\partial \mathbb{A}} :: \delta\mathbb{A} \\ =& ((1-a)(n+1)\mathbb{A}^n :: \delta\mathbb{A} + a(n+1)Tr[\mathbb{A}^n]Tr[\delta\mathbb{A}]) \\ & \frac{1}{n+1}\left((1-a)Tr[\mathbb{A}^{n+1}] + aTr[\mathbb{A}]^{n+1}\right)^{-\frac{n}{n+1}} \\ =& \frac{1}{z_m(\mathbb{A})^n}\left((1-a)\mathbb{A}'^n :: \delta\mathbb{A}' + aTr[\mathbb{A}']^n Tr[\delta\mathbb{A}']\right)\end{aligned}$$

Therefor the damage flow direction reads:

$$\frac{\partial z_m}{\partial \mathbb{A}} = \frac{1}{z_m(\mathbb{A})^n}\left((1-a)\mathbb{A}^n + aTr[\mathbb{A}]^n\mathbb{I}\right) \tag{52}$$

Note that:

$$\frac{\partial z_m}{\partial \mathbb{A}} :: \mathbb{A} = \frac{1}{z_m(\mathbb{A})^n}\left((1-a)Tr[\mathbb{A}^{n+1}] + aTr[\mathbb{A}]^{n+1}\mathbb{I}\right) = z_m(\mathbb{A}) \tag{53}$$

Acknowledgements

The author acknowledges Pr. R. Desmorat and Pr. P. Ladevèze from LMT-Cachan for their fruitful discussions and advices.

References

Aubard X (1992) *Modélisation et identification du comportement mécanique des matériaux composites 2D-C/SiC*. PhD Thesis, Thèse de doctorat: Paris VI.

Baranger E (2013) Building of a reduced constitutive law for ceramic matrix composites. *International Journal of Damage Mechanics* 22(8): 1222–1238.

Baranger E, Cluzel C, Ladevèze P and Mouret A (2008) Identification and validation of a multi-physic macro model for the lifetime prediction of self-healing ceramic matrix composites. In: *ECCM 13*. Stockholm.

Baranger E, Cluzel C, Ladevèze P and Mouret A (2011) Effects of the thermomechanical loading path on the lifetime prediction of self-healing ceramic matrix composites. *Science and Engineering of Composite Materials* 18(4): 259–264.

Bernachy-Barbé F (2014) *Caractérisation des mécanismes d'endommagement et modélisation du comportement mécanique sous chargements multi-axiaux de tubes composites SiC/SiC*. PhD Thesis, Paris, ENMP.

Bernachy-Barbe F, Gélébart L, Bornert M, Crépin J and Sauder C (2015a) Anisotropic damage behavior of SiC/SiC composite tubes: Multiaxial testing and damage characterization. *Composites Part A: Applied Science and Manufacturing* 76: 281–288.

Bernachy-Barbe F, Gélébart L, Bornert M, Crépin J and Sauder C (2015b) Characterization of SiC/SiC composites damage mechanisms using digital image correlation at the tow scale. *Composites Part A: Applied Science and Manufacturing* 68: 101–109.

Betten J (1983) Damage tensors in continuum mechanics. *Journal de Mecanique theorique et appliquee* 2(1): 13–32.

Carol I and Willam K (1996) Spurious energy dissipation/generation in stiffness recovery models for elastic degradation and damage. *International Journal of Solids and Structures* 33(20): 2939–2957.

Chaboche J (1977) Sur l'utilisation des variables détat interne pour la description du comportement viscoplastique et de la rupture par endommagement. In: *Proc. Problemes non-linéaires de mécanique, Symposium franco-polonais, Cracow (Poland)*. pp. 137–159.

Chaboche J (1982) Le concept de contrainte effective appliqué à l'élasticité et à la viscoplasticité en présence d'un endommagement anisotrope. In: *Mechanical Behavior of Anisotropic Solids/Comportment Méchanique des Solides Anisotropes*. Springer, pp. 737–760.

Chaboche J, Lesne P, Maire J and Office National d'Etudes et de Recherches Aerospatiales (ONERA) CF (1994) Phenomenological damage mechanics of brittle materials with description of unilateral damage effects. *Fracture and Damage in Quasibrittle Structures* : 75–84.

Chaboche J and Maire J (2001) New progress in micromechanics-based CDM models and their application to CMCs. *Composites Science and Technology* 61(15): 2239–2246.

Chaboche JL (1992) Damage induced anisotropy: on the difficulties associated with the active/passive unilateral condition. *International Journal of Damage Mechanics* 1(2): 148–171.

Cluzel C, Baranger E, Ladevèze P and Mouret A (2009) Mechanical behaviour and lifetime modelling of self-healing ceramic-matrix composites subjected to thermomechanical loading

in air. *Composites Part A: Applied Science and Manufacturing* 40(8): 976–984.

Cordebois J and Sidoroff F (1979) Anisotropie élastique induite par endommagement. *Comportement mécanique des solides anisotropes* (295): 761–774.

Cormery F and Welemane H (2002) A critical review of some damage models with unilateral effect. *Mechanics Research Communications* 29(5): 391–395.

Curnier A, He QC and Zysset P (1994) Conewise linear elastic materials. *Journal of Elasticity* 37(1): 1–38.

Desmorat R, Chambart M, Gatuingt F and Guilbaud D (2010) Delay-active damage versus non-local enhancement for anisotropic damage dynamics computations with alternated loading. *Engineering Fracture Mechanics* 77(12): 2294–2315.

Friderikos O and Baranger E (2016) Automatic building of a numerical simplified constitutive law for ceramic matrix composites using singular value decomposition. *International Journal of Damage Mechanics* 25(4): 506–537.

Gasser A, Ladeveze P and Poss M (1996) Damage mechanisms of a woven sicsic composite: Modelling and identification. *Composites science and technology* 56(7): 779–784.

Genet M, Marcin L, Baranger E, Cluzel C, Ladevèze P and Mouret A (2012) Computational prediction of the lifetime of self-healing CMC structures. *Composites Part A: Applied Science and Manufacturing* 43: 294–303. DOI:10.1016/j.compositesa.2011.11.004.

Genet M, Marcin L and Ladeveze P (2014) On structural computations until fracture based on an anisotropic and unilateral damage theory. *International Journal of Damage Mechanics* 23(4): 483–506.

Halm D and Dragon A (1998) An anisotropic model of damage and frictional sliding for brittle materials. *European Journal of Mechanics-A/Solids* 17(3): 439–460.

Ju J (1990) Isotropic and anisotropic damage variables in continuum damage mechanics. *Journal of Engineering Mechanics* 116(12): 2764–2770.

Kachanov L (1958) Time of the rupture process under creep conditions. *Isv. Akad. Nauk. SSR. Otd Tekh. Nauk* 8: 26–31.

Kachanov M (1992) Effective elastic properties of cracked solids: critical review of some basic concepts. *Applied Mechanics Reviews* 45(8): 304–335.

Ladeveze P (1983) On an anisotropic damage theory. *Proc. CNRS Int. Coll* 351: 355–363.

Ladevèze P (2002) *An anisotropic damage theory with unilateral effects: applications to laminates and to three-and four-dimensional composites*. O. Allix and F. Hild edition. Elsevier.

Ladevèze P, Baranger E, Genet M and Cluzel C (2014) *Ceramic Matrix Composites: Materials, Modeling and Technology*, chapter Damage and Lifetime Modeling for Structure Computations. John Wiley & Sons, Inc., pp. 465–519. N. P. Bansal and J. Lamon eds, ISBN: 978-1-118-23116-6, 712 pages.

Maire J and Lesne P (1997) A damage model for ceramic matrix composites. *Aerospace science and technology* 1(4): 259–266.

Maire J and Pacou D (1996) *Essais de traction-compression-torsion sur tubes composites céramique-céramique*.

Marcin L, Maire JF, Carrère N and Martin E (2011) Development of a macroscopic damage model for woven ceramic matrix composites. *International Journal of Damage Mechanics* 20(6):

939–957.

Murakami S (1988) Mechanical modeling of material damage. *Journal of Applied Mechanics* 55(2): 280–286.

Murakami S and Ohno N (1981) A continuum theory of creep and creep damage. In: *Creep in structures*. Springer, pp. 422–444.

Park T and Voyiadjis G (1998) Kinematic description of damage. *Journal of applied mechanics* 65(1): 93–98.

Rabotnov YN (1969) Creep rupture. In: *Applied mechanics*. Springer, pp. 342–349.

Voyiadjis G and Park T (1997) Anisotropic damage effect tensors for the symmetrization of the effective stress tensor. *Journal of Applied Mechanics* 64(1): 106–110.